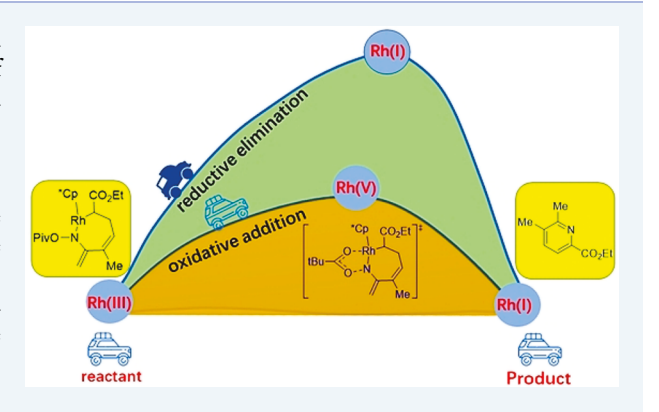


Origin of Regiochemical Control in Rh(III)/Rh(V)-Catalyzed Reactions of Unsaturated Oximes and Alkenes to Form Pyrdines

Yingzi Li,^{†,§} Haohua Chen,[‡] Ling-Bo Qu,[†] K. N. Houk,^{*,§} and Yu Lan^{*,†,‡}

Supporting Information

ABSTRACT: The Rh(III)-catalyzed reactions of α,β -unsaturated oximes with alkenes are versatile methods for the synthesis of pyridines. Density functional theory (DFT) calculations reported here reveal the detailed mechanism and origins of selectivity in this reaction. The Rh(III)/Rh(V)/Rh(I) catalytic cycle was found to be more favorable than the previously proposed Rh(III)/Rh(I)/ Rh(III) catalytic cycle. The Rh(III)/Rh(V)/Rh(I) catalytic cycle involves C-H activation, alkene insertion, deprotonation, oxime migratory oxidative addition, nitrene insertion, 1,5-hydrogen shift, and β -hydride elimination to give the pyridine product and form a Rh(I) species. Subsequent oxidation by Ag+ regenerates the Rh(III) catalyst. Reductive elimination from a alkyl-Rh(III) species is predicted to be difficult, so that the Rh(III)/Rh(I)/ Rh(III) catalytic cycle can be excluded. The reactivities of oxime



ethers and oxime esters are compared. The oxime ester acts as both a directing group and an internal oxidant. In this reaction, the N-O bond is activated by the pivalate, and migratory oxidative addition onto the Rh(III) species generates the corresponding Rh(V) nitrene complex. However, in the absence of the pivalate on the oxime ether, the activation energy for oxidative addition is much higher. The reactivity was analyzed by NPA charge calculations, comparison of the N-O bond orders, and the bond dissociation energies. The calculations also explain the regioselectivity of alkene insertion, which is shown to be an electronic effect rather than a steric effect.

KEYWORDS: regioselectivity, Rh(III)/Rh(V)-catalyzed, C-H activation, pyrdines, internal oxidant, Rh(V) nitrene

■ INTRODUCTION

Transition-metal-catalyzed C-H activation and functionalization are important tools for construction of new C-C and Cheteroatom bonds. 1-9 Rhodium catalysis is particularly valuable for such reactions. 10-16 The general mechanisms of Rh(III)-catalyzed C-H bond activation reactions have been thoroughly investigated by both calculations 17-23 and experiments. 10,11,24-27

Over the past two decades, many research groups have devoted effort to development of rhodium-catalyzed C-H bond activation reactions. 10-16,28 However, the mechanisms proposed for this type of reaction are not always clear. Some Rh(III)-catalyzed C-H activation reactions have long been considered to involve a Rh(III)/Rh(I) catalytic cycle, but there is not always sufficient evidence to support this mechanism.^{29–33} This type of reaction has generally been thought to proceed by deprotonation to generate an aryl-Rh(III) intermediate. Subsequent reductive elimination and oxidative addition can thus give the coupling product.32-34 Recently,

extensive and innovative studies have investigated Rh(III)catalyzed C-H functionalization. 10,14,24,35,36 When strong oxidative directing groups are used in rhodium catalysis, an alternative Rh(III)/Rh(V) catalytic cycle may be more favorable than the Rh(III)/Rh(I) catalytic cycle. Some Rh(V) intermediates and their generation/transformation have recently been investigated in depth by theoretical calculations, 37-40 and they have attracted interest from experimental chemists. For example, Xia et al.⁴¹ performed a detailed computational study of Rh(III)-catalyzed C-H functionalization of benzamine derivatives with alkenes. They found that the carbonyl oxygen of the oxime ester group can stabilize the rhodacycle such that a Rh(V)-nitrene complex forms resulting from pivalate migration from N to Rh. Wu and Houk⁴² reported a theoretical study of the Rh(III)-catalyzed

Received: May 20, 2019 Revised: June 27, 2019 Published: June 28, 2019



[†]College of Chemistry and Molecular Engineering, Zhengzhou University, Zhengzhou 450001, P. R. China

[‡]School of Chemistry and Chemical Engineering, and Chongqing Key Laboratory of Theoretical and Computational Chemistry, Chongqing University, Chongqing 400030, P. R. China

Department of Chemistry and Biochemistry, University of California—Los Angeles, Los Angeles, California 90095-1569, United States

redox coupling reaction of N-phenoxyacetamides with acetylenes. They elucidated the role of the internal oxidizing directing group and found that oxidative addition of the O–N bond occurs before reductive elimination. Therefore, the Rh(III)/Rh(V) catalytic cycle is an alternative catalytic cycle in Rh-catalyzed redox-neutral arene C–H functionalizations. Our group 21,43 has also reported some mechanistic studies of Rh(III)-catalyzed C–H functionalizations in which the catalytic cycle involves a Rh(V)–nitrene complex. However, there is still limited experimental evidence to support the high oxidation state of Rh(V) intermediates.

Many facile syntheses of diversely substituted pyridines have been reported in recent years, and Rh(III)-catalyzed oxidative cyclization of oxime derivatives followed by further functionalization provides a versatile tool for construction of these heterocycles. Recently, Rovis and co-workers 33,47 established the utility of rhodium catalysis for synthesis of multisubstituted pyridines from α , β -unsaturated oximes and substituted alkenes with good yield and regioselectivity (Scheme 1). The reaction of O-pivaloyl oxime 1 and ethyl

Scheme 1. Rhodium-Catalyzed Reactions of α,β -Unsaturated Oximes and Alkenes

acrylate 2 catalyzed by Cp*Rh(III) gives 6-substituted pyridines with 20:1 regioselectivity ratio (rr) and 92% yield. Using the O-methyl oxime derivative substrate, the pyridine product is not generated by Rh-catalyzed oxidative cyclization. In addition, carboxyl alkene 5 undergoes Rh(III)-catalyzed decarboxylative coupling with O-pivaloyl oximes to give 5-substituted pyridines with 20:1 rr. Rovis's group suggested that there is a steric component to control of the regioselectivity. When the reaction in Scheme 1 is performed with AcOD to 50% conversion, deuterium incorporation is observed at the α -position methyl group of 3. Several key experiments contributed to understanding the reaction mechanism, which is considered to be a Rh(III)/Rh(I) catalytic cycle.

The redox neutral strategy using various N–O bond containing oxidizing directing groups such as an N-oxide, N-acyloxy, N-methoxy, and O-pivaloyl group that can act as a directing group and internal oxidant have recently been developed. With this strategy, the oxidation of a low-valent metal by these internal oxidants will result in cleavage of an N–O bond and provide a high oxidation state species. The mechanisms for these Rh(III)-catalyzed reactions of α , β -unsaturated oximes and alkenes, as well as how the O-pivaloyl moiety acts as an internal oxidant are still unclear. In this study, we performed density functional theory (DFT) calculations to investigate the potential mechanisms by both the Rh(III)/Rh(I)/Rh(III) and Rh(III)/Rh(V)/Rh(I) catalytic cycles to understand how the type of internal oxidant (O-pivaloyl and

O-methyl) influences these transformations. DFT calculations were also performed to obtain insight into the origin of the observed regioselectivity.

■ COMPUTATIONAL METHODS

All the DFT calculations were carried out with the GAUSSIAN 09 series of programs. The B3LYP 53,54 functional was used for geometry optimizations at a standard basis set 6-31G(d) $^{55-57}$ (LANL2DZ $^{58-60}$ basis set for Rh). Harmonic vibrational frequency calculations were performed for all stationary points to confirm them as local minima or transition structure and to derive the thermochemical corrections for the enthalpies and free energies. The M06 functional proposed was used with a 6-311+G(d,p) 61 basis set (SDD 62,63 basis set for Rh atom) to calculate the single-point energies in the solvent. The solvent effects were considered by single-point calculations in dichloroethane solvent base on the gas-phase stationary points with SMD solvation model. The energies presented in this paper are the M06 calculated Gibbs free energies in dichloroethane solvent with B3LYP calculated thermodynamic corrections. (GM06 = Esolv-M06 + Gcorr-B3LYP).

RESULTS AND DISCUSSION

The proposed mechanism for rhodium-catalyzed reaction of $\alpha_1\beta$ -unsaturated oximes and alkenes is shown in Scheme 2. On

Scheme 2. Plausible Catalytic Cycles for Rhodium-Catalyzed Reactions of α,β -Unsaturated Oximes and Alkenes

the basis of previous theoretical studies of the mechanisms of rhodium-catalyzed C–H activation and other related reactions, cationic Cp*Rh(III) acetate complex **A** is regarded as the real catalyst, which can be generated from the [RhCp*Cl₂]₂ additive by chloride dissociation and ligand exchange in the presence of AgOAc. The initial C–H activation occurs by concerted-metalation deprotonation (CMD) to form Rh(III) metallacycle **B**, followed by alkene insertion to give seven-membered rhodacycle **C** (formally a 16-electron species). The oxime ester group in intermediate **C** is acidic.

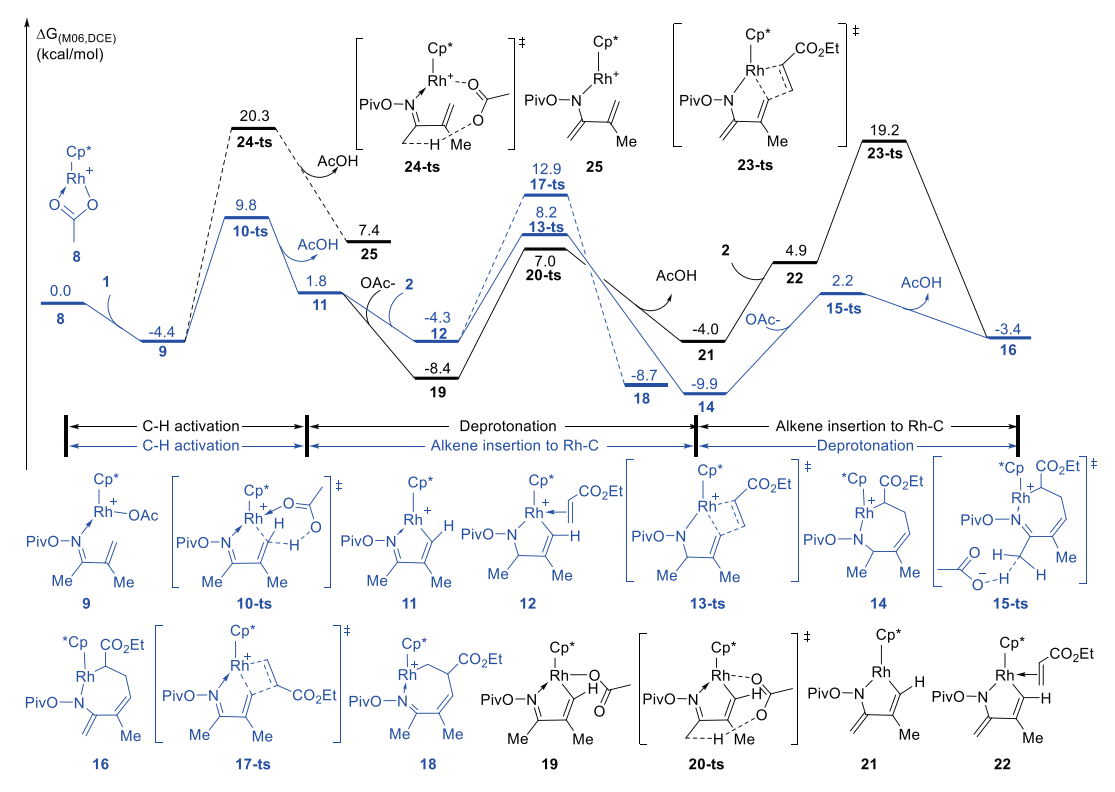


Figure 1. Gibbs energy profiles of C-H metalation and alkene insertion of rhodium-catalyzed reactions from O-pivaloyl oximes 1 and ethyl acrylate 2.

Therefore, deprotonation of the oxime α -hydrogen atom occurs in the presence of acetate as the base to form enamine rhodacycle **D**. With the common species **D** in hand, both the Rh(III)/Rh(I)/Rh(III) and Rh(III)/Rh(V)/Rh(I) catalytic cycles were considered, because the oxime group can act as an internal oxidant for this type of transformation. In path a (the Rh(III)/Rh(V)/Rh(I) catalytic cycle), oxidative addition to the O–N bond occurs and Rh(V) species **E** forms. Rh(V) nitrene **E** can then undergo C–N reductive elimination to form **F**. Subsequently, the corresponding 1,5-hydrogen shift could be isomerized to the Rh(III) complex **G**. β -Hydride elimination then gives product **P** and generates rhodium hydride species **H**, which can be oxidized by Ag(I) to regenerate active catalyst **A**.

The Rh(III)/Rh(I)/Rh(III) and Rh(III)/Rh(V)/Rh(I) catalytic cycle was also considered. In path b, common intermediate **D** undergoes β-hydride elimination to give rhodium hydride intermediate **J**. N–H bond reductive elimination then generates Rh(I) intermediate **E**. Oxidative addition of the N–O bond in the oxime group to Rh(I) followed by a 1,3-hydrogen shift generates rhodium ylideneamino **L**. Intramolecular nucleophilic attack by the amino group leads to cycloaddition with generation of intermediate **G**. Alternatively, in path c, reductive elimination of the C–N bond in intermediate **D** followed by oxidative addition of the N–O bond in intermediate **I** forms common species **F**.

On the basis of analysis of the reaction mechanism, we found that the competition between the Rh(III)/Rh(I)/Rh(III) and Rh(III)/Rh(V)/Rh(I) catalytic cycle is important for this reaction, which is difficult to determine experimentally. Moreover, C–H activation of the α , β -unsaturated oxime could occur at various points in the catalytic cycles. The question

arises, how does the *O*-pivaloyl substituent act as an internal oxidant to promote this reaction? In this respect, DFT calculations are a powerful tool to reveal the detailed reaction mechanism and to obtain deeper mechanistic insight into this type of reaction. Using these results, we will discuss and interpret the regioselectivity observed for the reactions of unsymmetrical alkenes.

The initiation of rhodium-catalyzed oxidative cyclization of α,β -unsaturated oximes and alkenes involves three steps: vinyl C–H activation, deprotonation of the oxime α -H atom, and alkene insertion. However, the order of these steps remains unclear

The M06 functional calculated Gibbs free energy profiles of the possible catalytic cycles for the initiation process are shown in Figure 1. In the theoretical calculations, the *O*-pivaloyl oxime 1 and ethyl acrylate 2 substrates were selected as model reactants, which can give 6-substituted pyridine 3 in the presence of a rhodium catalyst (Scheme 3). Cationic rhodium

Scheme 3. Rhodium-Catalyzed Reactions of $\alpha \beta$ -Unsaturated *O*-pivaloyl oxime 1 and ethyl acrylate 2

complex 8 was considered to be the active catalyst for the oxidative cyclization reaction, and the free energy of 8 was set as the baseline for the calculated free energy profiles.

Coordination of the oxime directing group in reactant 1 to form intermediate 9 is exergonic by 4.4 kcal/mol. CMD-type vinyl C-H bond cleavage then occurs via transition state 10-ts

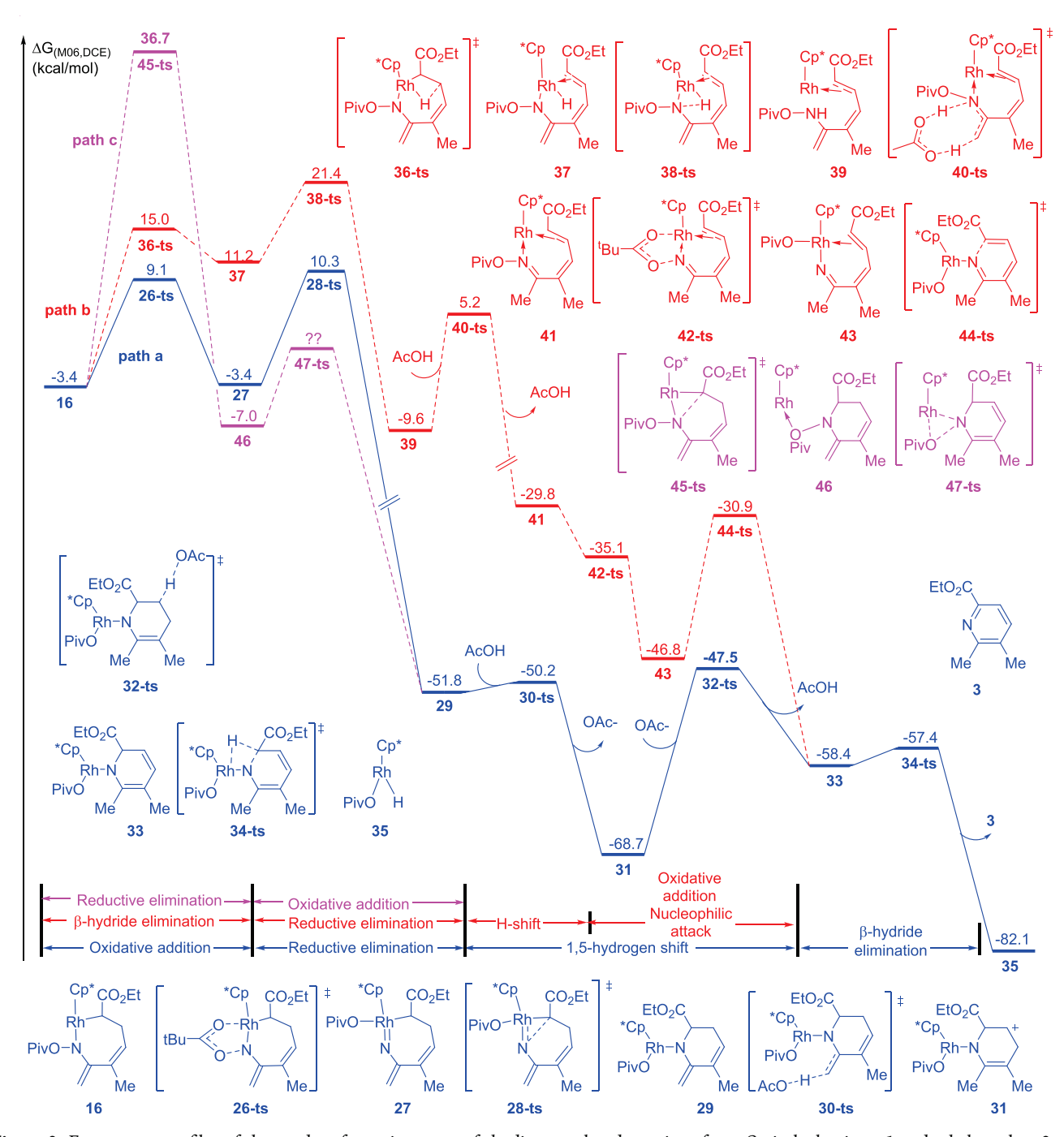


Figure 2. Free energy profiles of the product formation steps of rhodium-catalyzed reactions from O-pivaloyl oximes 1 and ethyl acrylate 2.

with a free energy barrier of 14.2 kcal/mol to reversibly form five-membered rhodacycle 11. C–H activation of the oxime α -carbon atom has a relative free energy of transition state 24-ts that is 10.5 kcal/mol higher than that of 10-ts, and can be excluded.

The order of alkene insertion and deprotonation of the oxime α -carbon atom for formation of intermediate 11 was also investigated by DFT calculations. As shown in Figure 1 (blue lines), coordination of ethyl acrylate 2 to generate intermediate 12 is exergonic by 6.1 kcal/mol. Alkene insertion occurs via transition state 13-ts with a free energy barrier of 12.5 kcal/mol from intermediate 12 to give cationic sevenmembered rhodacycle 14. Subsequent deprotonation of the oxime α -carbon atom proceeds with assistance of an extra

acetate ion via transition state **15-ts** to reversibly form common intermediate **16**. The calculated free energy barrier of this step is only 12.1 kcal/mol. This is consistent with isotopic labeling experiments, where deuterium incorporation was observed at the position of this methyl group when the reaction was performed with AcOD to 50% conversion.

Alternatively, deprotonation of the oxime α -carbon atom could occur before alkene insertion. The calculated relative free energy of transition state **20-ts** is 1.2 kcal/mol lower than that of **13-ts**, which reversibly forms enamino rhodacycle **21**. However, we found that the calculated free energy barrier of alkene insertion followed by deprotonation of the oxime α -carbon atom is 23.2 kcal/mol, which reveals that deprotonation is unfavorable for alkene insertion. The relative free energy

of 23-ts is 11.0 kcal/mol higher than that of 13-ts, so the reaction order is concluded to be vinyl C–H activation, alkene insertion, and deprotonation of the oxime α -carbon atom. The regioselectivity of the alkene was also considered for a substituted alkene. We found that the relative free energy of 17-ts is 4.7 kcal/mol higher than that of 13-ts, so generation of intermediate 14 is more rapid than generation of intermediate 18. The calculated regioselectivity agrees with experimental observations.

The mechanism of the subsequent annulation process was investigated. When seven-membered rhodacycle 16 forms, C-N reductive elimination could give a Rh(I) species. Alternatively, the N-O bond of the oxime moiety could act as an oxidant for the corresponding oxidative addition to form a Rh(V) species. Therefore, both the Rh(III)/Rh(I)/Rh(III) and Rh(III)/Rh(V)/Rh(I) catalytic cycles are possible in the following process. For path a (blue lines in Figure 2), oxidative addition of intermediate 16 leads to cleavage of the N-O bond via five-membered transition state 26-ts with an energy barrier of 12.5 kcal/mol to reversibly form neutral Rh(V) nitrene complex 27. Subsequent migratory insertion of nitrene into the Rh-C bond of this complex occurs via transition-state 28-ts with a small energy barrier of 13.7 kcal/mol to irreversibly form Rh(III)—amido complex 29 with release of 62.1 kcal/mol of free energy. Complex 29 could then isomerize to rhodium complex 33 by a 1,5-hydrogen shift with assistance of acetic acid. From 29, facile protonation by acetic acid occurs via transition state 30-ts with an activation energy of only 1.6 kcal/mol. Subsequent acetate-assisted deprotonation via transition state 32-ts generates pyridinyl-Rh(III) complex 33 with an activation free energy of 21.2 kcal/mol. Subsequent facile β -hydride elimination occurs via transition state 34-ts to give the corresponding 6-substituted pyridine product 3 and Rh-H species 35, which has a barrier of only 1.0 kcal/mol. Finally, the active Rh(III) catalyst is generated from the Rh-H species by further oxidation by Ag(I).

The previously proposed Rh(III)/Rh(I)/Rh(III) catalytic cycle was also considered. As shown in Figure 2, it also starts from neutral species 16. In path b (red lines), β -hydride elimination occurs via transition state 36-ts to form Rh(III) hydride 37 with an activation free energy of 18.4 kcal/mol. Subsequent reductive elimination of the N-H bond via transition state 38-ts gives olefin-coordinated Rh(I) complex 39. The overall activation free energy of this process from intermediate 14 is 31.3 kcal/mol. Subsequently, in the presence of acetate, the enamine moiety in complex 39 irreversibly isomerizes to an imine species 41 via transition state 40-ts with an activation free energy of 14.8 kcal/mol. Sequential oxidative addition occurs via transition state 42-ts without an energy barrier. Subsequent reductive elimination with an activation free energy of 15.9 kcal/mol gives pyridinyl-Rh(III) complex 33. Comparison of paths a and b reveals that the relative free energy of transition state 38-ts is 11.1 kcal/ mol higher than that of transition state 28-ts, indicating that path a is favorable. In an alternative Rh(III)/Rh(I) pathway (path c, pink lines), reductive elimination from species 16 occurs via transition state 45-ts form the C-N bond to give Rh(I) species 46. The activation energy of this step is an enormous 45.6 kcal/mol. The results indicate that path c is unlikely because of its extremely high activation energy, and this pathway would not occur under mild conditions.

To compare the Rh(III)/Rh(I)/Rh(III) and Rh(III)/Rh(V)/Rh(I) catalytic cycles for formation of pyridine product

3, the key transition states of the possible transformations are shown in Figure 3. Seven-membered rhodacycle 16 containing

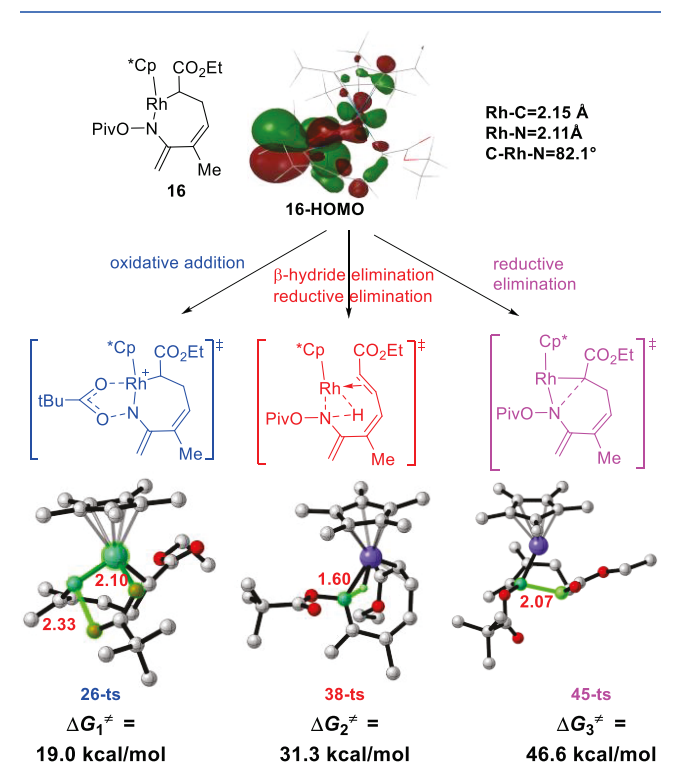


Figure 3. Key intermediate and transition states for competition between the Rh(III)/Rh(I) and Rh(III)/Rh(V) catalytic cycles in rhodium-catalyzed reactions of O-pivaloyl oximes 1 and ethyl acrylate 2. Hydrogen atoms except for the transferring proton are omitted for clarity.

an pivaloyl oxime moiety acts as an oxidizing directing group that cleaves the O-N bond to form the Rh(V)-nitrene complex. The calculated activation free energy for intramolecular oxidative addition of the O-N bond to Rh(III) via transition state 26-ts is 12.3 and 27.6 kcal/mol lower than that of reductive elimination via transition states 36-ts and 45-ts. respectively. Therefore, the annulation process would occur by the Rh(III)/Rh(V)/Rh(I) catalytic cycle. Direct reductive elimination of 16-electron Rh(III) intermediate 16 to form a new C-N bond from the cyclic alkyl amino Rh(III) species is difficult. However, formal reduction of 18-electron Rh(V)nitrene complex 27 is facile, which can be considered to be nitrene migratory insertion into the alkyl-Rh bond. This result is similar to a previous study by Houk's group, 42 who found that C-N formation by reductive elimination of the C(sp3)-Rh(III)-N unit is more difficult than that by reductive elimination of the C(sp3)-Rh(V)-N unit. The bond orders of the Rh-C and Rh-N bonds in Rh(III) intermediate 16 are determined to be 0.60 and 0.48 by natural population analysis (NPA), which indicate that the Rh-C and Rh-N bonds are strong. The frontier molecular orbitals (FMOs) of intermediate 16 were also calculated, and they are shown in Figure 3. The highest occupied molecular orbital of intermediate 16 is located in the bonding orbital of the $d\pi$ -p π back-donation bond of the Rh-N bond, which indicates that the Rh-N bonds are strengthened by a $d\pi-p\pi$ back-donation interaction. This result suggests the low reactivity of the C-N reductive

elimination could be attributed to the strength of the breaking Rh-N bond.

Experimentally, when crotonic acid 5 is used as the reactant, 5-substituted pyridine 6 is obtained as the main product by decarboxylation with good regionselectivity (Scheme 4). DFT

Scheme 4. Rhodium-Catalyzed Reactions of α,β -Unsaturated O-Pivaloyl Oxime 1 and Crotonic Acid 5

calculations were also performed to investigate the mechanism and regioselectivity of rhodium-catalyzed oxidative cyclization

of α , β -unsaturated oximes and crotonic acid (Figure 4). The common starting intermediate 11 forms by acetate-assisted electrophilic deprotonation, and alkene insertion into the Rh–C bond forms a new C–C bond. There are two competitive olefin insertion modes in the following process. Alkene insertion occures via transition state 49-ts with an activation free energy of 15.7 kcal/mol to form seven-membered rhodacycle 50. Alternatively, alkene insertion could occur via transition state 51-ts. The relative free energy of transition state 49-ts is 7.7 kcal/mol higher than that of 51-ts, indicating that it is a kinetically unfavorable process. From rhodacycle 50, intermolecular deprotonation of the carboxyl moiety by acetate via transition state 53-ts with an activation energy of 20.4 kcal/mol gives acetoxyrhodium complex 54.

The corresponding Rh(III)/Rh(I)/Rh(III) and Rh(III)/Rh(V)/Rh(I) catalytic cycles for formation of pyridine product

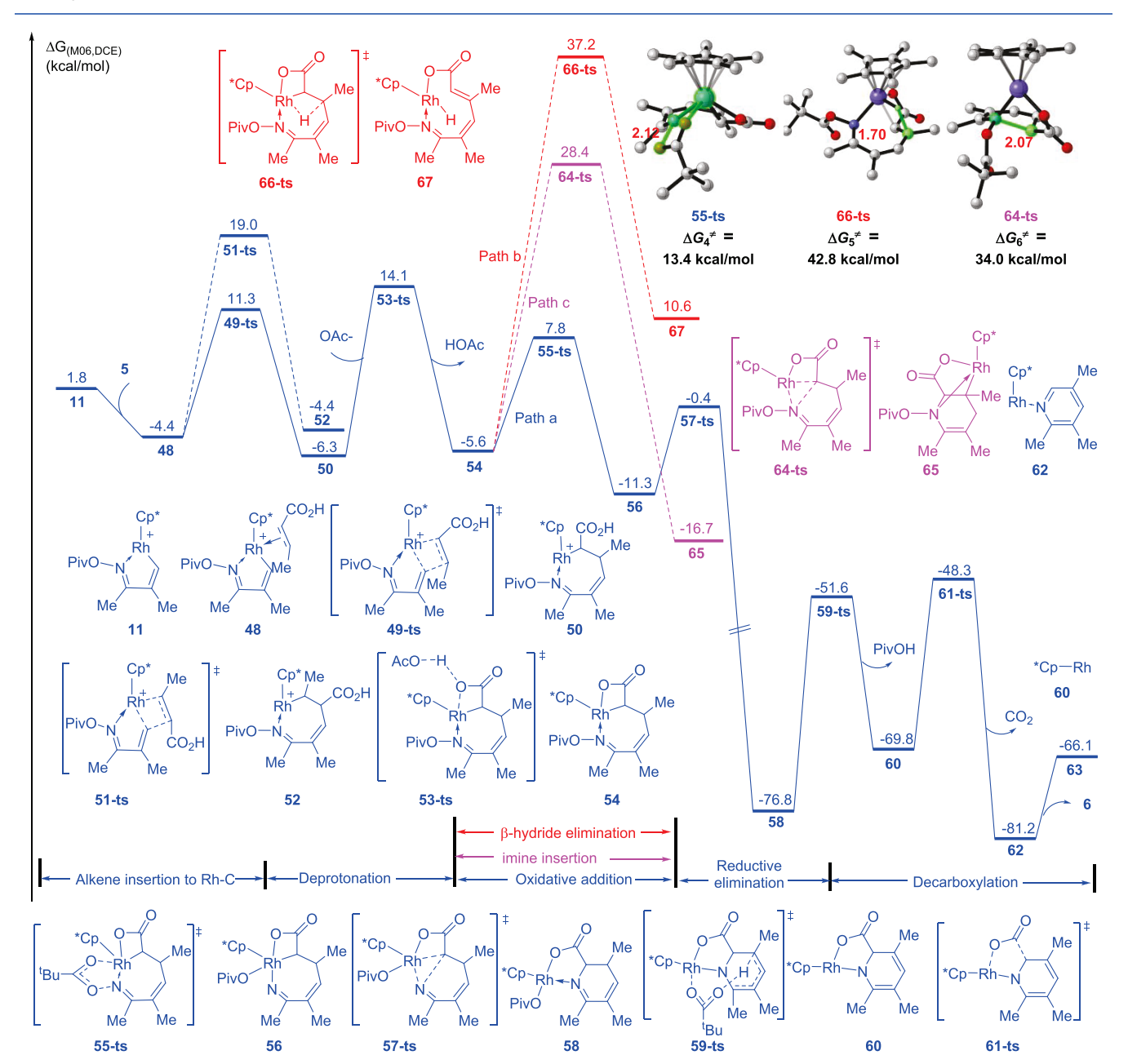


Figure 4. Gibbs energy profiles of Rh-catalyzed reactions of O-pivaloyl oximes 1 and crotonic acid 5 for formation of decarboxylated pyridines.

6 from complex **54** were also considered. In path a, N–O bond oxidative addition occurs via transition state **55-ts** to form high-valence Rh(V)—eneamino complex **56** with an energy barrier of 13.4 kcal/mol. C–N bond formation of 18-electron Rh(V) **56** then occurs via C(sp3)—Rh(V)—N unit reductive elimination transition state **57-ts** with an energy barrier of 11.7 kcal/mol, leading to irreversible generation of dihydropyridine-coordinated Rh(III) species **58**. Subsequent intramolecular deprotonation by pivalate occurs via transition state **59-ts** with an activation energy of 25.2 kcal/mol. The 5-substituted pyridine **6** species forms by decarboxylation via transition state **61-ts**. The overall activation free energy of decarboxylation is 28.5 kcal/mol.

In path b, β -H elimination of Rh(III) intermediate 54 via transition state 66-ts gives a Rh(III) hydride complex, which has an energy barrier of 42.8 kcal/mol. The relative free energy of 66-ts is 29.4 kcal/mol higher than that of transition state 55ts. On the basis of these data, β -H elimination is unlikely because of its extremely high activation energy. In addition, C-N bond formation of intermediate 54 could occur by intramolecular imine migration insertion into the alkyl-Rh bond via transition state 64-ts with an activation free energy of 34.0 kcal/mol. The results show that C-N bond formation from the C(sp3)-Rh(III)-N unit is still difficult in this process. The geometry of transition state 64-ts shows that it is the resulting broken conjugation between the imine and the alkene moiety with C-N bond formation that leads to the higher activation energy. Thus, the Rh(III)/Rh(V) catalytic cycle is the favorable reaction pathway for rhodium-catalyzed decarboxylated reactions of α,β -unsaturated oximes and crotonic acid.

Experimentally, Rovis's group^{33,47} found that when an oxime ether is used as the reactant instead of an oxime ester, the corresponding oxidative cyclization for construction of pyridine does not occur (Scheme 5). We will attempted to

Scheme 5. Rhodium-Catalyzed Reactions of α,β -Unsaturated O-Methyl Oxime 68 and Ethyl Acrylate 2

explain the difference of reactivity for this Rh-catalyzed oxidative cyclization reaction. As shown in Figure 5, according to the corresponding steps with the oxime ester reactant, seven-membered rhodacycle 76 can be generated by C-H activation via 70-ts, alkene insertion via 73-ts, and deprotonation via 75-ts. The calculated activation energies for these steps are analogous to the corresponding steps with an oxime ester reactant. In path a, the calculated activation free energy for intramolecular oxidation of Rh(III) species 76 to Rh(V) species 86 by the oxime ether internal oxidant via threemembered ring transition state 85-ts is 49.6 kcal/mol. Therefore, the reaction cannot occur along the Rh(III)/ Rh(V) catalytic cycle. Reductive elimination of 76 to form the C-N bond via transition state 87-ts is also not possible because of the high relative free energy of 52.4 kcal/mol. In path c, β -H elimination from the corresponding sevenmembered rhodacycle 76 requires an activation barrier of 14.7 kcal/mol. Subsequent N-H bond reductive elimination of the generated Rh hydride intermediate 78 is more difficult

than β -H elimination. The calculated overall activation free energy is 34.5 kcal/mol (from intermediate 74 to transition state 79-ts). Thus, the Rh(III)/Rh(I) catalytic cycle can also be excluded. This result shows why the pyridine product does not form using oxime ether substrates under typical reaction conditions. The computational results are consistent with the experimental observations.

The calculated activation free energy for oxidative addition of the O–N bond of 16 to form Rh(V) species via transition state 26-ts is only 12.5 kcal/mol. In contrast to the oxime ester moiety, the oxidizability of the oxime ether group to give a Rh(V) species is significantly more difficult. To understand the difference between the oxidizabilities of the oxime ester and oxime ether, the NPA charge distributions and N–O bond orders of these two compounds and the corresponding Rh species were calculated. As shown in Figure 6, the bond order of the N–O bond in 16 is 0.87, while it is 0.94 in 76. The calculated bond orders indicate that the covalent N–O bond in complex 16 becomes weaker with coordination to Rh.

The bond orders and bond lengths of the N-O bonds illustrate the ester moiety is a much better leaving group than the ether moiety. In addition, when the corresponding oximes are coordinated to Rh in complexes 16 and 76, the NPA charges of the nitrogen atoms are similar, but the negative charge on the oxygen atom of the coordinated oxime ester (-0.42) is somewhat lower than that of the coordinated oxime ether (-0.47). The lower negative charge can be attributed to the extra coordination of the ester moiety to Rh, which leads to donation of negative charge from the oxygen atom of the oxime ester and N-O bond easily broken. Therefore, the oxidizability of the oxime ester is stronger than that of the oxime ether.

To further reveal the difference of the reactivity between the oxime ester and the oxime ether, scans of the relative energies with respect to the N-O bond length for oxime ester 1, oxime ether 68, and the corresponding coordination intermediates 16 and 76 are shown in Figure 7. It clearly shows that when the length of corresponding N-O bond increases, the relative energy of the compounds also increases. The rate of increase of the energy for oxime ester 1 is significantly lower than that for oxime ether 68, which indicates that the oxime can be activated by the function of the ester group. We also found that coordination to Rh can activate the corresponding N-O bond. As shown in Figure 7, the slopes for complexes 16 and 76 are significantly lower than those for complexes 1 and 68, respectively. Therefore, with activation of the ester group and coordination to Rh, the N-O bond in complex 16 is further activated, which can be broken by oxidative addition to Rh. The DFT calculations reveal that oxidative addition is promoted by the oxime ester moiety in this reaction.

DFT calculations were performed to understand the regioselectivity of rhodium-catalyzed reactions of α,β -unsaturated oximes and alkenes. On the basis of the proposed mechanism, the regioselectivity of this reaction is controlled by the alkene insertion step, which is determined by electronic as well as steric factors. ^{20,68} The optimized geometries and Gibbs energies of the alkene insertion transition states are shown in Figure 8. The relative free energy of transition state 13-ts is 3.1 kcal/mol lower than that of 17-ts. The structures for these two transition states show that the preferential coupling of the Rh center with the alkene does not originate from the steric effect. Therefore, we performed NPA to investigate the electronic effect. The NPA charges of carbon atoms C2 and C3 of ethyl

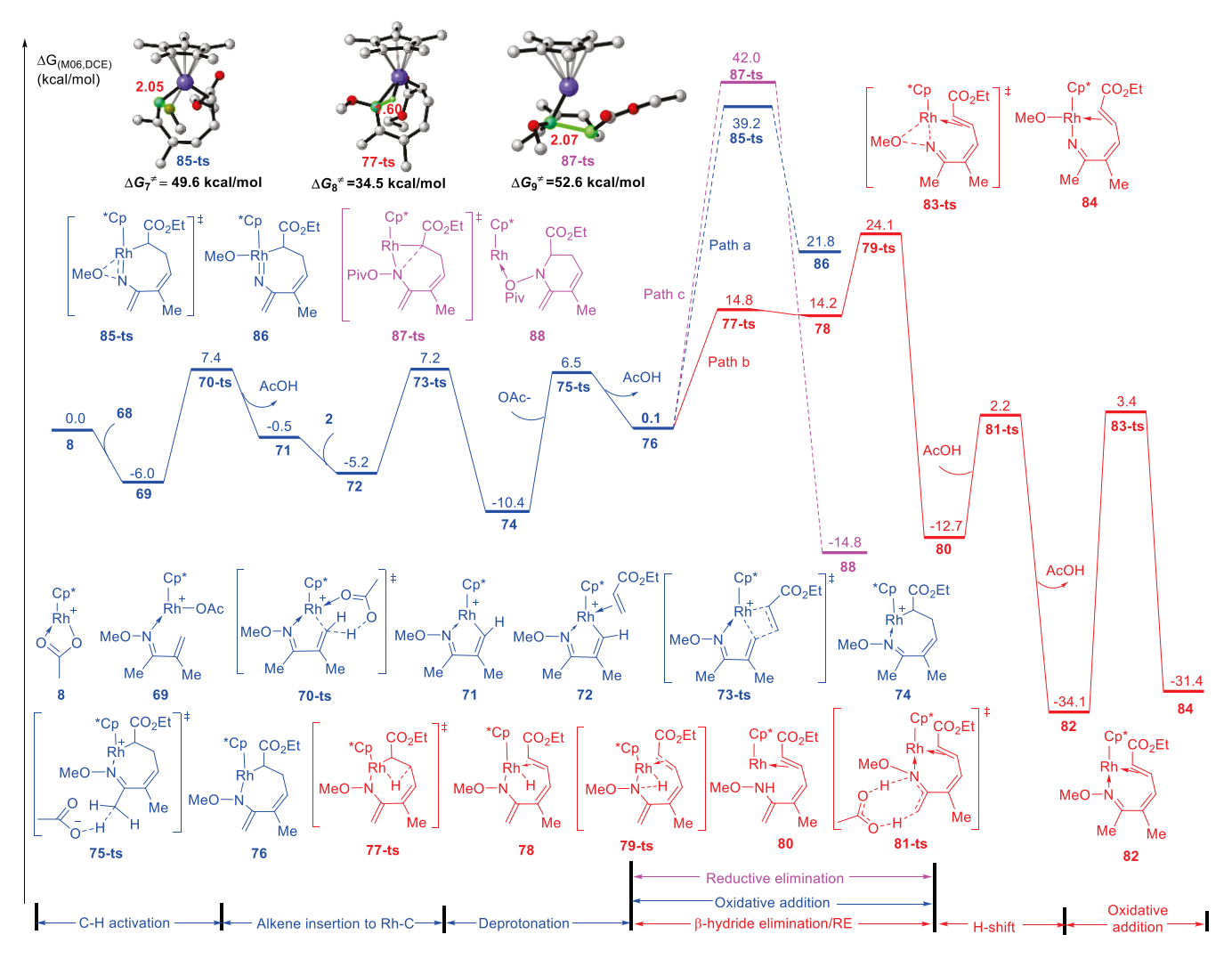


Figure 5. Gibbs energy profiles of the product formation steps of rhodium-catalyzed reactions from O-methyl oximes 68 and ethyl acrylate 2.

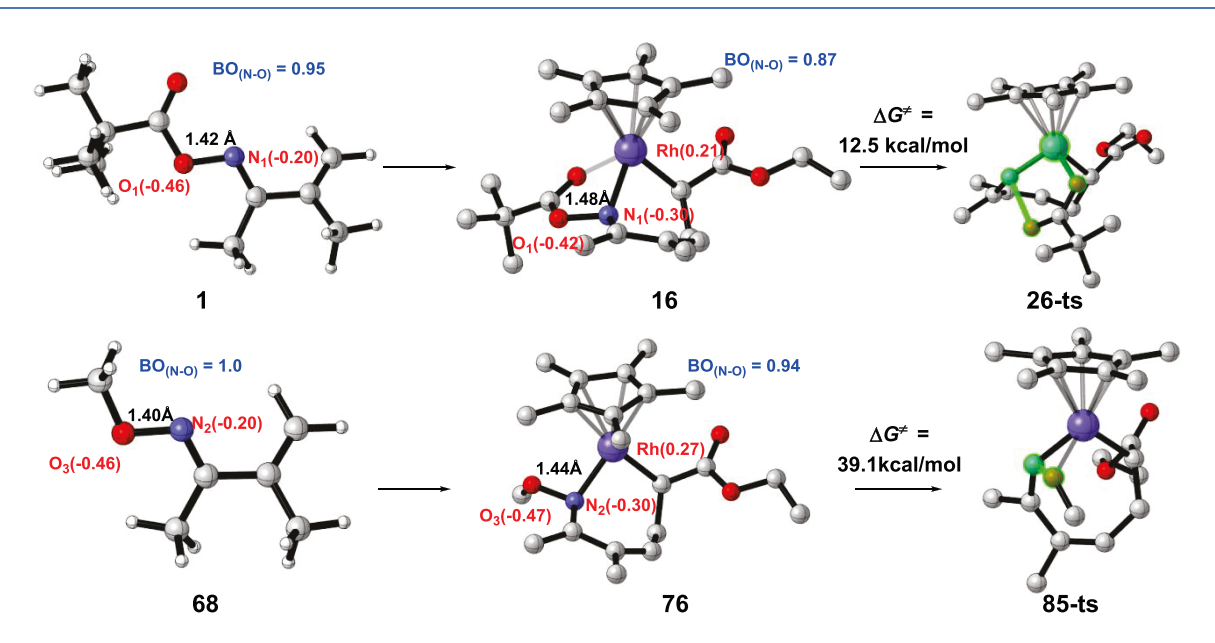


Figure 6. Optimized structures with the charge distributions and N-O bond orders for 1, 16, 26-ts, 68, 76, and 85-ts. The bond lengths are given in angstroms.

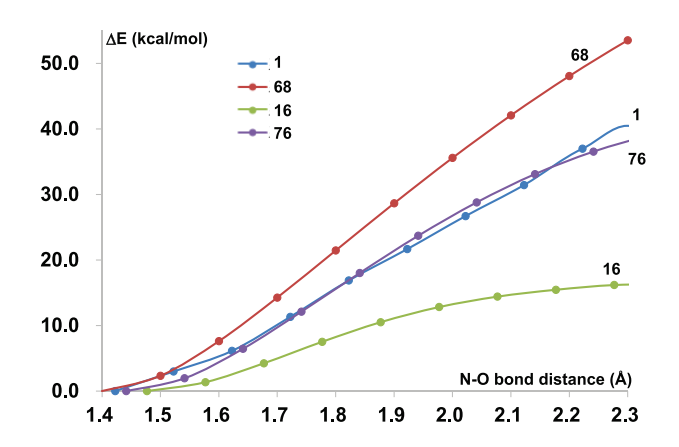


Figure 7. Scans of the bond dissociation energies of oxime ester 1, oxime ether 68, and the corresponding coordination intermediates 16 and 76.

acrylate 2 are -0.32 and -0.28, respectively, which indicates that the nucleophilicity of C2 is higher than that of C3. Therefore, formation of a Rh–C bond by nucleophilic attack of the higher nucleophilicity C2 carbon atom to the Rh (0.21) center is easier than that of the C3 carbon atom. When the carboxyl alkene 5 substrate is used, and the relative free energy of 49-ts is 7.7 kcal/mol lower than that of 51-ts. The NBO charge of the C4 carbon atom of 5 is -0.36, while that of the C5 carbon atom is only -0.06. Thus, the lower reaction barrier via transition state 49-ts can be attributed to the electronic interaction between the electrophilic Rh center of complex 11 and the C4 carbon atom of ethyl acrylate 5. The calculated

results show that the electronic properties influence regioselectivity control in the reaction.

CONCLUSIONS

The mechanism of Rh(III)-catalyzed reactions of α,β unsaturated oximes and alkenes has been revealed by DFT calculations. The Rh(III)/Rh(V)/Rh(I) catalytic cycle is more favorable than the previously proposed Rh(III)/Rh(I)/Rh(III) catalytic cycle. The theoretical calculations show that Rh(III)catalyzed reactions starts with oxime-directed CMD-type C-H bond cleavage of the α,β -unsaturated oxime, alkene insertion into the vinyl-Rh bond, and base-assisted deprotonation to form a seven-membered rhodacycle. Subsequent migratory oxidative addition of the N-O bond in the oxime ester gives a Rh(V)-nitrene complex, which can undergo nitrene insertion into the alkyl-Rh bond to form a pyridine ring. A 1,5hydrogen shift and β -hydride elimination then gives the pyridine product. The Rh(I) species is then oxidized by Ag(I)to regenerate the Rh(III) active catalyst. The theoretical calculations show that reductive elimination from an alkyl-Rh(III) species is difficult, so the Rh(III)/Rh(I)/Rh(III) catalytic cycle can be excluded. FMO analysis indicates that the Rh-N bond in complex 16 is strengthened by a $d\pi-p\pi$ backdonation interaction. We also found that when acrylic acid is used as the substrate instead of its ester, decarboxylation can occur through a five-membered-ring transition state.

The DFT calculations show that the type of internal oxidant (oxime ether or oxime ester) influences the reactivity of this oxidative cyclization reaction. The oxime ester acts as both a directing group and an internal oxidant. In this reaction, the N–O bond can be activated by the ester group, so migratory

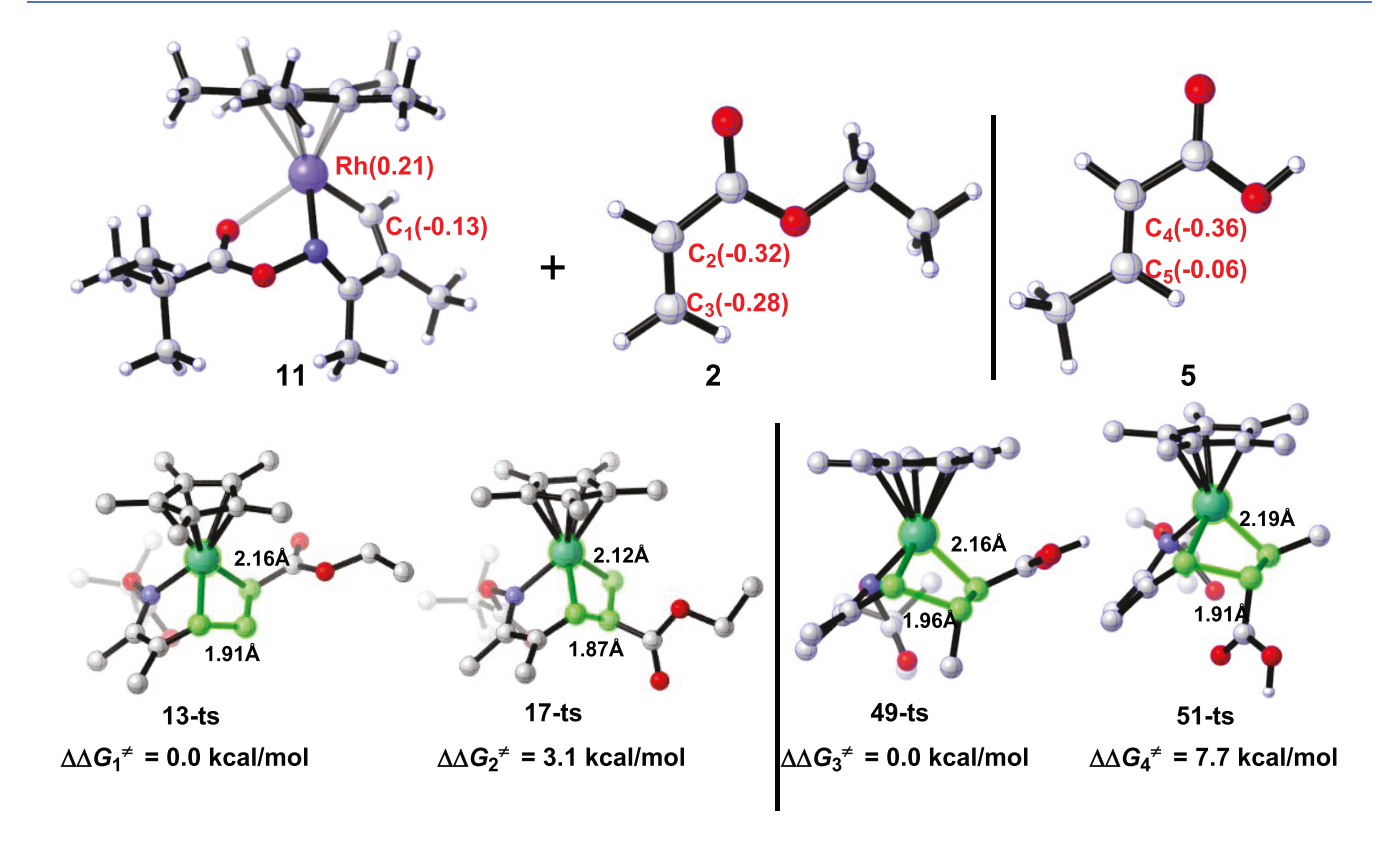


Figure 8. Optimized geometries and Gibbs energies of the alkene insertion transition states. The values in parentheses are the corresponding NPA charges of the atoms.

oxidative addition into the Rh(III) species can generate the corresponding Rh(V)—nitrene complex. However, in the absence of an ester group in the oxime ether, the activation energy for oxidative addition is much higher. The reactivity can be predicted by NPA charge calculations, comparison of the N–O bond orders, and the bond dissociation energies.

The regioselectivity was also investigated. The results show that the electronic properties influence regioselectivity control of the reaction. A DFT study could enable better understanding of the reaction and determine the wider synthetic applications of this methodology.

ASSOCIATED CONTENT

S Supporting Information

The Supporting Information is available free of charge on the ACS Publications website at DOI: 10.1021/acscatal.9b02085.

Cartesian coordinates and energies of all reported structures and full authorship of Gaussian 09 (PDF)

AUTHOR INFORMATION

Corresponding Authors

*E-mail: houk@chem.ucla.edu. *E-mail: lanyu@cqu.edu.cn.

ORCID ®

K. N. Houk: 0000-0002-8387-5261 Yu Lan: 0000-0002-2328-0020

Author Contributions

The manuscript was written through contributions of all authors. All authors have given approval to the final version of the manuscript.

Notes

The authors declare no competing financial interest.

ACKNOWLEDGMENTS

This project was supported by the National Science Foundation of China (Grants 21822303 and 21772020) and National Science Foundation of the U.S.A. (CHE-1361104 and CHE-1764328 to K.N.H.). We are also grateful to Fundamental Research Funds for the Central Universities (Chongqing University) (No. 2018CDXZ0002; 2018CDPTCG0001/4).

REFERENCES

- (1) Giri, R.; Shi, B. F.; Engle, K. M.; Maugel, N.; Yu, J.-Q. Transition metal-catalyzed C-H activation reactions: diastereoselectivity and enantioselectivity. *Chem. Soc. Rev.* **2009**, *38*, 3242–3272.
- (2) Lyons, T. W.; Sanford, M. S. Palladium-catalyzed ligand-directed C-H functionalization reactions. *Chem. Rev.* **2010**, *110*, 1147–1169.
- (3) Ackermann, L. Carboxylate-assisted transition-metal-catalyzed C-H bond functionalizations: mechanism and scope. *Chem. Rev.* **2011**, *111*, 1315–1345.
- (4) Ritleng, V.; Sirlin, C.; Pfeffer, M. Ru-, Rh-, and Pd-Catalyzed C-C Bond Formation Involving C-H Activation and Addition on Unsaturated Substrates: Reactions and Mechanistic Aspects. *Chem. Rev.* 2002, 102, 1731–1770.
- (5) Gutekunst, W. R.; Baran, P. S. C-H functionalization logic in total synthesis. *Chem. Soc. Rev.* **2011**, *40*, 1976–1991.
- (6) Wencel-Delord, J.; Glorius, F. C-H bond activation enables the rapid construction and late-stage diversification of functional molecules. *Nat. Chem.* **2013**, *5*, 369–375.
- (7) Liu, C.; Liu, D.; Lei, A. Recent advances of transition-metal catalyzed radical oxidative cross-couplings. *Acc. Chem. Res.* **2014**, *47*, 3459–3470.

(8) He, C.; Gaunt, M. J. Ligand-Enabled Catalytic C-H Arylation of Aliphatic Amines by a Four-Membered-Ring Cyclopalladation Pathway. *Angew. Chem., Int. Ed.* **2015**, *54*, 15840–15844.

- (9) Shan, C.; Zhu, L.; Qu, L. B.; Bai, R.; Lan, Y. Mechanistic view of Ru-catalyzed C-H bond activation and functionalization: computational advances. *Chem. Soc. Rev.* **2018**, *47*, 7552–7576.
- (10) Chen, J.; Song, G.; Pan, C. L.; Li, X. Rh(III)-catalyzed oxidative coupling of N-aryl-2-aminopyridine with alkynes and alkenes. *Org. Lett.* **2010**, *12*, 5426–5429.
- (11) Colby, D. A.; Tsai, A. S.; Bergman, R. G.; Ellman, J. A. Rhodium catalyzed chelation-assisted C-H bond functionalization reactions. *Acc. Chem. Res.* **2012**, *45*, 814–825.
- (12) Dateer, R. B.; Chang, S. Selective Cyclization of Arylnitrones to Indolines under External Oxidant-Free Conditions: Dual Role of Rh(III) Catalyst in the C-H Activation and Oxygen Atom Transfer. *J. Am. Chem. Soc.* **2015**, 137, 4908–4911.
- (13) Sharma, U.; Park, Y.; Chang, S. Rh(III)-catalyzed traceless coupling of quinoline N-oxides with internal diarylalkynes. *J. Org. Chem.* **2014**, *79*, 9899–9906.
- (14) Zhang, X.; Qi, Z.; Li, X. Rhodium(III)-catalyzed C-C and C-O coupling of quinoline N-oxides with alkynes: combination of C-H activation with O-atom transfer. *Angew. Chem., Int. Ed.* **2014**, 53, 10794–10798.
- (15) Gridnev, I. D.; Imamoto, T. On the mechanism of stereoselection in Rh-catalyzed asymmetric hydrogenation: a general approach for predicting the sense of enantioselectivity. *Acc. Chem. Res.* **2004**, *37*, 633–644.
- (16) Lewis, J. C.; Bergman, R. G.; Ellman, J. A. Direct functionalization of nitrogen heterocycles via Rh-catalyzed C-H bond activation. *Acc. Chem. Res.* **2008**, *41*, 1013–1025.
- (17) Chen, W.-J.; Lin, Z. Rhodium(III)-Catalyzed Hydrazine-Directed C-H Activation for Indole Synthesis: Mechanism and Role of Internal Oxidant Probed by DFT Studies. *Organometallics* **2015**, 34, 309–318.
- (18) Sperger, T.; Sanhueza, I. A.; Kalvet, I.; Schoenebeck, F. Computational Studies of Synthetically Relevant Homogeneous Organometallic Catalysis Involving Ni, Pd, Ir, and Rh: An Overview of Commonly Employed DFT Methods and Mechanistic Insights. *Chem. Rev.* **2015**, *115*, 9532–9586.
- (19) Li, Y.; Liu, S.; Qi, Z.; Qi, X.; Li, X.; Lan, Y. The Mechanism of N-O Bond Cleavage in Rhodium-Catalyzed C-H Bond Functionalization of Quinoline N-oxides with Alkynes: A Computational Study. *Chem. Eur. J.* **2015**, *21*, 10131–10137.
- (20) Li, Y.; Shan, C.; Yang, Y. F.; Shi, F.; Qi, X.; Houk, K. N.; Lan, Y. Mechanism, Regio-, and Diastereoselectivity of Rh(III)-Catalyzed Cyclization Reactions of N-Arylnitrones with Alkynes: A Density Functional Theory Study. *J. Phys. Chem. A* **2017**, *121*, 4496–4504.
- (21) Liu, S.; Qi, X.; Qu, L.-B.; Bai, R.; Lan, Y. C-H bond cleavage occurring on a Rh(v) intermediate: a theoretical study of Rh-catalyzed arene azidation. *Catal. Sci. Technol.* **2018**, *8*, 1645–1651.
- (22) Qi, X.; Li, Y.; Bai, R.; Lan, Y. Mechanism of Rhodium-Catalyzed C-H Functionalization: Advances in Theoretical Investigation. *Acc. Chem. Res.* **2017**, *50*, 2799–2808.
- (23) Lin, Y.; Zhu, L.; Lan, Y.; Rao, Y. Development of a Rhodium(II)-Catalyzed Chemoselective C(sp(3))-H Oxygenation. *Chem. Eur. J.* **2015**, 21, 14937–14942.
- (24) Guimond, N.; Gorelsky, S. I.; Fagnou, K. Rhodium(III)-catalyzed heterocycle synthesis using an internal oxidant: improved reactivity and mechanistic studies. *J. Am. Chem. Soc.* **2011**, *133*, 6449–6457.
- (25) Shi, Z.; Koester, D. C.; Boultadakis-Arapinis, M.; Glorius, F. Rh(III)-catalyzed synthesis of multisubstituted isoquinoline and pyridine N-oxides from oximes and diazo compounds. *J. Am. Chem. Soc.* 2013, 135, 12204–12207.
- (26) Yang, X.; Liu, S.; Yu, S.; Kong, L.; Lan, Y.; Li, X. Redox-Neutral Access to Isoquinolinones via Rhodium(III)-Catalyzed Annulations of O-Pivaloyl Oximes with Ketenes. *Org. Lett.* **2018**, *20*, 2698–2701.
- (27) Wang, X.; Li, Y.; Knecht, T.; Daniliuc, C. G.; Houk, K. N.; Glorius, F. Unprecedented Dearomatized Spirocyclopropane in a

Sequential Rhodium(III)-Catalyzed C-H Activation and Rearrangement Reaction. *Angew. Chem., Int. Ed.* **2018**, *57*, 5520–5524.

- (28) Ackermann, L.; Novak, P.; Vicente, R.; Hofmann, N. Ruthenium-catalyzed regioselective direct alkylation of arenes with unactivated alkyl halides through C-H bond cleavage. *Angew. Chem., Int. Ed.* **2009**, *48*, 6045–6048.
- (29) Xia, Y.; Liu, Z.; Liu, Z.; Ge, R.; Ye, F.; Hossain, M.; Zhang, Y.; Wang, J. Formal carbene insertion into C-C bond: Rh(I)-catalyzed reaction of benzocyclobutenols with diazoesters. *J. Am. Chem. Soc.* **2014**, *136*, 3013–3015.
- (30) Yu, S.; Li, X. Mild Synthesis of Chalcones via Rhodium(III)-Catalyzed C-C Coupling of Arenes and Cyclopropenones. *Org. Lett.* **2014**, *16*, 1220–1223.
- (31) Zhang, X.-S.; Chen, K.; Shi, Z.-J. Transition metal-catalyzed direct nucleophilic addition of C-H bonds to carbon-heteroatom double bonds. *Chem. Sci.* **2014**, *5*, 2146–2159.
- (32) Feng, C.; Loh, T. P. Rhodium-catalyzed C-H alkynylation of arenes at room temperature. *Angew. Chem., Int. Ed.* **2014**, *53*, 2722–2726
- (33) Neely, J. M.; Rovis, T. Rh(III)-catalyzed decarboxylative coupling of acrylic acids with unsaturated oxime esters: carboxylic acids serve as traceless activators. *J. Am. Chem. Soc.* **2014**, *136*, 2735–2738.
- (34) Ding, L.; Ishida, N.; Murakami, M.; Morokuma, K. sp3-sp2 vs sp3-sp3 C-C site selectivity in Rh-catalyzed ring opening of benzocyclobutenol: a DFT study. *J. Am. Chem. Soc.* **2014**, *136*, 169–178
- (35) Zhen, W.; Wang, F.; Zhao, M.; Du, Z.; Li, X. Rhodium(III)-Catalyzed Oxidative C—H Functionalization of Azomethine Ylides. *Angew. Chem.* **2012**, *124*, 11989–11993.
- (36) Too, P. C.; Wang, Y. F.; Chiba, S. Rhodium(III)-catalyzed synthesis of isoquinolines from aryl ketone O-acyloxime derivatives and internal alkynes. *Org. Lett.* **2010**, *12*, 5688–5691.
- (37) Collins, K. D.; Lied, F.; Glorius, F. Preparation of conjugated 1,3-enynes by Rh(III)-catalysed alkynylation of alkenes via C-H activation. *Chem. Commun.* **2014**, *50*, 4459–4461.
- (38) Guo, W.; Zhou, T.; Xia, Y. Mechanistic Understanding of the Aryl-Dependent Ring Formations in Rh(III)-Catalyzed C-H Activation/Cycloaddition of Benzamides and Methylenecyclopropanes by DFT Calculations. *Organometallics* **2015**, *34*, 3012–3020.
- (39) Park, S. H.; Kwak, J.; Shin, K.; Ryu, J.; Park, Y.; Chang, S. Mechanistic studies of the rhodium-catalyzed direct C-H amination reaction using azides as the nitrogen source. *J. Am. Chem. Soc.* **2014**, 136, 2492–2502.
- (40) Zhou, T.; Guo, W.; Xia, Y. Rh(V) -Nitrenoid as a Key Intermediate in Rh(III)-Catalyzed Heterocyclization by C-H Activation: A Computational Perspective on the Cycloaddition of Benzamide and Diazo Compounds. *Chem. Eur. J.* **2015**, 21, 9209–
- (41) Xu, L.; Zhu, Q.; Huang, G.; Cheng, B.; Xia, Y. Computational elucidation of the internal oxidant-controlled reaction pathways in Rh(III)-catalyzed aromatic C-H functionalization. *J. Org. Chem.* **2012**, 77. 3017–3024.
- (42) Yang, Y. F.; Houk, K. N.; Wu, Y. D. Computational Exploration of Rh(III)/Rh(V) and Rh(III)/Rh(I) Catalysis in Rhodium(III)-Catalyzed C-H Activation Reactions of N-Phenoxyacetamides with Alkynes. J. Am. Chem. Soc. 2016, 138, 6861–6868.
- (43) Zhang, T.; Qi, X.; Liu, S.; Bai, R.; Liu, C.; Lan, Y. Computational Investigation of the Role Played by Rhodium(V) in the Rhodium(III)-Catalyzed ortho-Bromination of Arenes. *Chem. Eur. J.* **2017**, 23, 2690–2699.
- (44) Colby, D. A.; Bergman, R. G.; Ellman, J. A. Synthesis of dihydropyridines and pyridines from imines and alkynes via C-H activation. *J. Am. Chem. Soc.* **2008**, *130*, 3645–3651.
- (45) Hyster, T. K.; Rovis, T. Pyridine synthesis from oximes and alkynes via rhodium(III) catalysis: Cp* and Cp(t) provide complementary selectivity. *Chem. Commun.* (Cambridge, U. K.) **2011**, 47, 11846–11848.

- (46) Too, P. C.; Chua, S. H.; Wong, S. H.; Chiba, S. Synthesis of azaheterocycles from aryl ketone O-acetyl oximes and internal alkynes by Cu-Rh bimetallic relay catalysts. *J. Org. Chem.* **2011**, *76*, 6159–6168
- (47) Neely, J. M.; Rovis, T. Rh(III)-catalyzed regioselective synthesis of pyridines from alkenes and alpha, beta-unsaturated oxime esters. *J. Am. Chem. Soc.* **2013**, *135*, 66–69.
- (48) Liu, G.; Shen, Y.; Zhou, Z.; Lu, X. Rhodium(III)-catalyzed redox-neutral coupling of N-phenoxyacetamides and alkynes with tunable selectivity. *Angew. Chem., Int. Ed.* **2013**, *52*, 6033–6037.
- (49) Patureau, F. W.; Glorius, F. Oxidizing directing groups enable efficient and innovative C-H activation reactions. *Angew. Chem., Int. Ed.* **2011**, *50*, 1977–1979.
- (50) Tan, Y.; Hartwig, J. F. Palladium-catalyzed amination of aromatic C-H bonds with oxime esters. *J. Am. Chem. Soc.* **2010**, *132*, 3676–3677.
- (51) Yoo, E. J.; Ma, S.; Mei, T. S.; Chan, K. S.; Yu, J. Q. Pd-catalyzed intermolecular C-H amination with alkylamines. *J. Am. Chem. Soc.* **2011**, *133*, 7652–7655.
- (52) Frisch, M. J.; Trucks, G. W.; Schlegel, H. B.; Scuseria, G. E.; Robb, M. A.; Cheeseman, J. R.; Scalmani, G.; Barone, V.; Mennucci, B.; Petersson, G. A.; Nakatsuji, H.; Caricato, M.; Li, X.; Hratchian, H. P.; Izmaylov, A. F.; Bloino, J.; Zheng, G.; Sonnenberg, J. L.; Hada, M.; Ehara, M.; Toyota, K.; Fukuda, R.; Hasegawa, J.; Ishida, M.; Nakajima, T.; Honda, Y.; Kitao, O.; Nakai, H.; Vreven, T.; Montgomery, J. A., Jr.; Peralta, J. E.; Ogliaro, F.; Bearpark, M.; Heyd, J. J.; Brothers, E.; Kudin, K. N.; Staroverov, V. N.; Kobayashi, R.; Normand, J.; Raghavachari, K.; Rendell, A.; Burant, J. C.; Iyengar, S. S.; Tomasi, J.; Cossi, M.; Rega, N.; Millam, N. J.; Klene, M.; Knox, J. E.; Cross, J. B.; Bakken, V.; Adamo, C.; Jaramillo, J.; Gomperts, R.; Stratmann, R. E.; Yazyev, O.; Austin, A. J.; Cammi, R.; Pomelli, C.; Ochterski, J. W.; Martin, R. L.; Morokuma, K.; Zakrzewski, V. G.; Voth, G. A.; Salvador, P.; Dannenberg, J. J.; Dapprich, S.; Daniels, A. D.; Farkas, Ö.; Foresman, J. B.; Ortiz, J. V.; Cioslowski, J.; Fox, D. J. Gaussian 09, revision D.01; Gaussian, Inc.: Wallingford, CT, 2013.
- (53) Becke, A. D. Density-functional thermochemistry. III. The role of exact exchange. *J. Chem. Phys.* **1993**, *98*, 5648–5652.
- (54) Lee, C.; Yang, W.; Parr, R. G. Development of the Colle-Salvetti correlation-energy formula into a functional of the electron density. *Phys. Rev. B: Condens. Matter Mater. Phys.* **1988**, 37, 785–789.
- (55) Ditchfield, R.; Hehre, W. J.; Pople, J. A. Self-Consistent Molecular-Orbital Methods. IX. An Extended Gaussian-Type Basis for Molecular-Orbital Studies of Organic Molecules. *J. Chem. Phys.* **1971**, 54, 724–728.
- (56) Hariharan, P. C.; Pople, J. A. The influence of polarization functions on molecular orbital hydrogenation energies. *Theor. Chim. Acta.* 1973, 28, 213–222.
- (57) Hehre, W. J.; Ditchfield, R.; Pople, J. A. SelfConsistent Molecular Orbital Methods. XII. Further Extensions of GaussianType Basis Sets for Use in Molecular Orbital Studies of Organic Molecules. *J. Chem. Phys.* **1972**, *56*, 2257–2261.
- (58) Cruz, V. L.; Muñoz-Escalona, A.; Martinez-Salazar, J. Ab initio calculation of ethylene insertion in zirconocene catalyst systems: A comparative study between bridged and unbridged complexes. *Polymer* **1996**, *37*, 1663–1667.
- (59) Ehlers, A. W.; Böhme, M.; Dapprich, S.; Gobbi, A.; Höllwarth, A.; Jonas, V.; Köhler, K. F.; Stegmann, R.; Veldkamp, A.; Frenking, G. A set of f-polarization functions for pseudo-potential basis sets of the transition metals Sc-Cu, Y-Ag and La-Au. *Chem. Phys. Lett.* **1993**, 208, 111–114
- (60) Roy, L. E.; Hay, P. J.; Martin, R. L. Revised Basis Sets for the LANL Effective Core Potentials. *J. Chem. Theory Comput.* **2008**, 4, 1029–1031.
- (61) Krishnan, R.; Binkley, J. S.; Seeger, R.; Pople, J. A. Self-consistent molecular orbital methods. XX. A basis set for correlated wave functions. *J. Chem. Phys.* **1980**, 72, 650–654.
- (62) Andrae, D.; Haussermann, U.; Dolg, M.; Stoll, H.; Preuss, H. Energy-adjustedab initio pseudopotentials for the second and third row transition elements. *Theor. Chim. Acta.* **1990**, *77*, 123–141.

(63) Dolg, M.; Wedig, U.; Stoll, H.; Preuss, H. Energy-adjusted ab initio pseudopotentials for the first row transition elements. *J. Chem. Phys.* **1987**, *86*, *866*–*872*.

- (64) Marenich, A. V.; Cramer, C. J.; Truhlar, D. G. Universal solvation model based on solute electron density and on a continuum model of the solvent defined by the bulk dielectric constant and atomic surface tensions. *J. Phys. Chem. B* **2009**, *113*, 6378–6396.
- (65) Yu, S.; Liu, S.; Lan, Y.; Wan, B.; Li, X. Rhodium-catalyzed C-H activation of phenacyl ammonium salts assisted by an oxidizing C-N bond: a combination of experimental and theoretical studies. *J. Am. Chem. Soc.* **2015**, *137*, 1623–1631.
- (66) Brasse, M.; Campora, J.; Ellman, J. A.; Bergman, R. G. Mechanistic study of the oxidative coupling of styrene with 2-phenylpyridine derivatives catalyzed by cationic rhodium(III) via C-H activation. *J. Am. Chem. Soc.* **2013**, *135*, 6427–6430.
- (67) Liu, L.; Wu, Y.; Wang, T.; Gao, X.; Zhu, J.; Zhao, Y. Mechanism, reactivity, and selectivity in Rh(III)-catalyzed phosphoryl-directed oxidative C-H activation/cyclization: a DFT study. *J. Org. Chem.* **2014**, *79*, 5074–5081.
- (68) Guimond, N.; Fagnou, K. Isoquinoline synthesis via rhodium-catalyzed oxidative cross-coupling/cyclization of aryl aldimines and alkynes. *J. Am. Chem. Soc.* **2009**, *131*, 12050–12051.